Article Type (Communication)

The Impact of Donor-Acceptor Phase Separation on the Charge Carrier Dynamics in pBTTT:PCBM Photovoltaic Blends[a]

Dominik W. Gehrig, Ian A. Howard, Sean Sweetnam, Tim M. Burke, Michael D. McGehee, Frédéric Laquai*

————

D. W. Gehrig, Dr. F. Laquai
Max Planck Research Group for Organic Optoelectronics, Max Planck Institute for Polymer Research, Ackermannweg 10, D-55128 Mainz, Germany
E-mail: laquai@mpip-mainz.mpg.de

Assoc. Prof. F. Laquai
present address: Physical Sciences and Engineering Division (PSE), Material Science and Engineering (MSE), Solar and Photovoltaics Engineering Research Center (SPERC), King Abdullah University of Science and Technology (KAUST), Thuwal 23955-6900, Kingdom of Saudi Arabia
E-mail: frederic.laquai@kaust.edu.sa

Dr. I. A. Howard
Institute of Microstructure Technology (IMT), Karlsruhe Institute of Technology (KIT), Hermann-von-Helmholtz-Platz 1, D-76344 Eggenstein-Leopoldshafen, Germany

S. Sweetnam, T. M. Burke, Prof. M. D. McGehee
Materials Science and Engineering, Stanford University, 476 Lomita Mall, Stanford, California, 94305-4045, USA

————

We present the effect of donor-acceptor phase separation, controlled by the donor-acceptor mixing ratio, on the charge generation and recombination dynamics in pBTTT-C14:$PC_{70}BM$ bulk heterojunction photovoltaic blends. Transient absorption (TA) spectroscopy spanning the dynamic range from pico- to microseconds in the visible and near-infrared spectral regions reveals that in a 1:1 blend exciton dissociation is ultrafast, however, charges cannot entirely escape their mutual Coulomb attraction and thus predominantly recombine geminately on a sub-ns timescale. In contrast, a polymer:fullerene mixing ratio of 1:4 facilitates the formation

---

of spatially-separated, that is free, charges and reduces substantially the fraction of geminate charge recombination, in turn leading to much more efficient photovoltaic devices. This illustrates that spatially-extended donor or acceptor domains are required for the separation of charges on an ultrafast timescale (<100 fs), indicating that they are not only important for efficient charge transport and extraction, but also critically influence the initial stages of free charge carrier formation.

1. Introduction

The growing global demand of energy is a major challenge that motivates the search for sustainable solutions for energy production, which satisfy requirements including long-term availability as well as economic and ecological constraints. Amongst the variety of renewable energy sources, organic photovoltaics are a promising and steadily developing technology. Recently, single-junction solar cells have been demonstrated with power conversion efficiencies exceeding 10%, thus approaching the efficiency of amorphous silicon solar cells.[1, 2] However, a proper choice of processing conditions is required to reach optimum performance of each material system. The most often used layout is a bulk heterojunction (BHJ) organic solar cell consisting of intermixed phases of an electron donor (D) and acceptor (A) material. Upon absorption of a photon a tightly bound exciton is created in the photoactive layer, which can be split into free charges at the D-A interface, a process driven by the energy offset between the energy levels of the two components.[3] However, the mechanism of charge separation is still debated and thought to depend on parameters such as the crystallinity and extent of the donor[4-6] and acceptor domains[7, 8], the conjugation length of the polymeric donor[9], the charge carrier mobility of the single components[10] and the orientation of donor and acceptor molecules with respect to each other.[11, 12] Free charges created at the interface upon exciton dissociation are collected at the electrodes after transport in the donor and acceptor networks, however, they are prone to non-geminate recombination

during transport prior to extraction. In fact, a large interfacial area ensures virtually quantitative exciton dissociation, however, it simultaneously increases recombination, if the interface is not well-connected to the bulk materials as charge carriers cannot escape their mutual attraction. Thus, finding the optimum morphology is a complex optimization problem and a tradeoff exists between maximizing the D-A interface, where charge separation occurs, and the optimization of percolation pathways that allow for efficient separation and charge carrier collection. Recent literature provides more insight into these complex relations between the donor-acceptor phase separation and the efficiency of charge generation, however, an entirely conclusive picture has not been developed yet.[7, 13-16]

Changing the donor and acceptor ratio is one important parameter to control the phase separation, aggregation, and crystallinity of the blend. Its tuning is critical for the optimization of many BHJ systems. This has been very precisely studied in blends of the donor polymer poly[2,5-bis(3-tetradecylthiophen-2-yl)thieno[3,2-b]thiophene] (pBTTT-C14) and the fullerene derivative $PC_{70}BM$. Specifically, specular X-Ray diffraction demonstrated that PCBM intercalates between the side chains of pBTTT-C16, thereby creating a well-defined cocrystal at blending ratios of 1:1.[17] However, at increased fullerene fractions the acceptor molecules cannot all be accommodated in the cocrystal phase anymore, and thus extended PCBM domains are additionally created.

This clear and well characterized morphology makes pBTTT an ideal system to study the photophysics of charge generation in strongly intermixed (cocrystal) and phase-separated (high fullerene-loading) conditions. It was recently shown that an excess of $PC_{60}BM$ (D:A = 1:3) yields a higher fraction of long-lived (> 1.5 ns) charges in contrast to samples with a 1:1 donor-acceptor ratio.[18] A separate study on pBTTT and other donor polymers suggested that charge generation is limited to the intermixed phases of donor and acceptor.[16] Very recently, Zusan *et al*. showed that charge separation is less field-dependent in a 1:4 blend of pBTTT:$PC_{61}BM$ compared to a 1:1 composition and concluded that pure and spatially-

extended fullerene domains facilitate field-independent charge separation.[19] It has also been found that there is an energetic offset between the mixed and pure phases that enhances separation of electrons and holes into free carriers.[7, 20-23] In the following we present the charge carrier dynamics in pBTTT:PC$_{70}$BM (see **Chart 1** for chemical structures) for 1:1 blends that exclusively contain the cocrystal phase and 1:4 blends that contain both the cocrystal phase and extended fullerene clusters. Precisely, we demonstrate by pico- to microsecond broadband transient absorption pump-probe spectroscopy, an all-optical technique complementary to the electro-optical experiments recently presented by Zusan et al.,[19] that the improvement of the photovoltaic performance with higher than 1:1 fullerene loadings is a consequence of the generation of spatially-separated, that is free, charges, while in the cocrystal (D:A = 1:1) sub-ns geminate recombination dominates the photophysics in turn significantly limiting the device performance. This illustrates that extended PCBM domains play a role in the generation and spatial separation of charges on an ultrafast timescale, showing that they are not only important for charge extraction, but also critically influence the initial stages of free charge formation very well in line with the recently reported results of Zusan et al.[19]

2. Experimental Section

The preparation of the organic solar cells is described in detail in the supplementary material. Spectroscopic samples were prepared by spincoating the active layer on quartz substrates with a donor-acceptor ratio of 1:1(c/c) and 1:4(w/w), respectively. Our transient absorption spectroscopy setup has been described earlier[24] and additional information can be found in the supplementary material.[25]

3. Results and Discussion

Table 1 shows the figures of merit of solar cells made with the two different donor-acceptor blending ratios. The 1:1 blend exhibits a rather poor photovoltaic efficiency of 0.55%, while the 1:4 blend exhibits a moderate power conversion efficiency of 2.4%, largely due to an improved short circuit current. The current-voltage characteristics of the respective devices are shown in **Figure S1**.

The sub-ns TA spectra of the blends are presented in **Figure 1(a)**. The samples were excited at a wavelength of 520 nm, which excites both the polymer as well as the fullerene. The spectra of both blends exhibit a ground-state bleaching (GSB) below 650 nm and a photo-induced absorption (PA) spanning the spectral range from 650 nm up to ~1200 nm. No photo-induced absorption could be observed beyond 1200 nm at time delays greater than 1 ps. The TA spectra show two remarkable differences. Firstly, the ratio of the two peaks of the ground-state bleaching changes with the donor-acceptor ratio. While in the 1:1 blend the peak at 616 nm is more pronounced than the peak at 572 nm, the situation is reversed in the 1:4 blend, in which the peak at 614 nm is smaller than the one at 567 nm. Secondly, the 1:4 sample shows a distinct peak at 647 nm, which is not present in the 1:1 sample. Both observations can be explained by the phenomenon of electro-absorption (EA) occurring at the donor-acceptor interface as reported recently for other polymer:fullerene blends.[26] EA is caused by the presence of an electric field across the donor-acceptor interface itself created by the presence of oppositely charged carriers sufficiently close to the interface to create a local electric field across it. The local electric field shifts the ground state absorption spectrum of nearby polymer molecules, effectively leading to a first derivative shape of the transient absorption spectrum in the region of the ground state bleaching [see **Figure S2(b)**]. In fact, a superposition of the thin film absorption and the first derivative of the absorption [**Figure S2(c)**] matches the measured spectrum of the 1:4 blend at early times and explains the change in the ground-state bleaching as well as the feature observed at 647 nm very well.

The observation of a pronounced EA in the 1:4 blend and its absence in the 1:1 blend indicates that in the 1:4 blend spatial separation of charge carriers occurs, that in turn create a local electric field across the interface that affects the absorption of nearby polymer molecules, while in the 1:1 blend, in which the EA feature is absent, charges appear to be trapped close to the interface, thereby limiting the spatial extension of the electric field to a small volume in between the two carriers. The presence of these EA features in the 1:4 blend from the earliest times onwards also suggests that the carrier separation is ultrafast.[26] A further analysis of the intensity-dependent kinetics is shown in **Figure 1(b)**, **S3(a)** and **S3(b)**. Firstly, the evolution of the pBTTT ground-state bleaching after excitation of the donor as well as acceptor molecules is analyzed. The maximum signal amplitude in the 1:1 blend is observed directly after photoexcitation, and the spectra resemble the same shape as time progresses. This implies ultrafast charge transfer from $PC_{70}BM$ to pBTTT and vice versa taking place on the sub-100 fs timescale. Given the intercalation of fullerene molecules between the side chains of the polymer backbone, it appears that excitons are always created close to the donor-acceptor interface, and hence ultrafast charge generation is facilitated. After the exciton dissociation, a fast and intensity-independent signal decay is observed indicating that the excited-state population consists mostly of geminate pairs that quickly recombine at the interface to the ground state by geminate recombination.

In contrast, the 1:4 blend shows a steady rise of the polymer's ground-state bleaching up to several tens of picoseconds. This indicates that exciton dissociation in this system is not exclusively ultrafast, but that a fraction of exciton dissociation is diffusion-limited, likely because excitons created in fullerene-rich domains must travel to the interface. The rise time observed depends on the excitation intensity, a consequence of exciton-charge and exciton-exciton annihilation in the fullerene domains at higher excitation intensities. These observations are in line with the formation of large, polymer-free domains of PCBM molecules within the photoactive layer of the 1:4 blend.

The rate of electron transfer from the pBTTT to the fullerene can be qualitatively assessed by looking at the pBTTT exciton-induced absorption in the spectral region above 1200 nm. Tracking the dynamics in this wavelength region reveals a signal decaying on a sub-picosecond timescale [**Figure S3(b)**]. This indicates that in both samples, namely the 1:1 and 1:4 blend, the pBTTT polymer exciton does not have to diffuse prior to electron transfer to an acceptor molecule, because the polymer exciton is generated in the cocrystal, where all polymer sites are located at a polymer:fullerene interface, while in the 1:4 blend a fraction of the photogenerated fullerene excitons diffuse prior to exciton dissociation.

The kinetics of the charge-induced absorption signal in the 1055-1075 nm spectral region support our analysis of the GSB. In the 1:1 sample the charge-induced absorption decays to about 10% of the initial value within 1 ns independent of the excitation intensity. This is consistent with the decay of the GSB, indicating geminate recombination of charges. The 1:4 blend on the other hand shows a diffusion-limited rise of the charge-induced absorption signal in line with a rise of the GSB. At longer delay times the intensity-dependent decay of the charge-induced absorption and GSB of the 1:4 blend are consistent with non-geminate recombination of free charges as discussed in more detail below.

To sum up the aforementioned results of the ps-ns TA experiments, we observed ultrafast exciton dissociation in the 1:1 blend followed by a significant amount of sub-ns geminate recombination of charges, while in the 1:4 blend ultrafast plus diffusion-limited exciton dissociation and charge formation is observed, and charge carriers are initially separated over a significantly larger distance as indicated by a pronounced EA signal at around 650 nm and by the intensity dependent carrier dynamics. Our results support recent findings presented by Zusan et al.,[19] who demonstrated by time-delayed collection field experiments that the field dependence of charge separation in pBTTT-C_{16}:$PC_{60}BM$ is much more pronounced in 1:1 blends than in 1:4 blends indicating less spatial separation of charges upon charge transfer in

the former compared to the latter and highlighting the importance of extended and pure fullerene domains for efficient charge separation.

We now turn to the results obtained on longer timescales, that is ns-μs measurements of the 1:1 and 1:4 blends. The dynamics in this time range reveals the recombination of longer-lived charge carriers. The respective TA spectra and decay dynamics of the GSB are shown in **Figure 2**. In the 1:1 blend we primarily observe recombination of charges following a decay process that does not depend on the excitation intensity or charge carrier density pointing to geminate and trap-assisted recombination. In contrast the 1:4 blend exhibits intensity-dependent dynamics associated with non-geminate recombination of free charges.

The short (ps-ns) and long-time (ns-μs) decay dynamics of the 1:1 blend can be very well approximated by a mono-exponential fit [see **Figure 3(a)**] including an offset. The data collected on the sub-ns and the ns-μs timescales are both fitted with a single exponential resulting in inverse decay rates of 221 ps and 1.39 ns, respectively, the latter likely being a convolution of the signal decay and temporal resolution of our ns-μs TA setup limited by the ns pulse width of the pump laser. These decays account for 68-75% of the total signal decay in the 1:1 blend. The remaining signal decays in an intensity-independent manner, indicating trap-assisted recombination and / or recombination of long-lived charge-transfer states. In fact, intensity-independent recombination on the ns-μs time scale was previously demonstrated by Durrant and coworkers in polymer:ICBA blends and assigned to loosely-bound polaron pairs.[21]

The charge carrier dynamics of the 1:4 blend was fitted by a two-pool model considering two separate non-interacting pools of charges generated on a sub-ns timescale, the first pool decaying by a single exponential process accounting for geminate recombination and the second pool by non-geminate recombination of free charge carriers.[27] We determine that in the 1:4 blend about 10 % of the charges undergo geminate recombination with a rate of ~1 ns, while 90% of the decay on the ns-μs timescale can be assigned to free charge recombination

following non-geminate and thus intensity-dependent recombination dynamics. The effective non-geminate recombination coefficient at a charge carrier concentration of 5×10^{15} cm^{-3}, which is relevant for solar illumination conditions, was calculated to be 9.11×10^{-13} cm^{3}s^{-1} and is comparable to that measured in other polymer:PCBM systems previously reported by us such as PCDTBT:PC$_{60}$BM and P3HT:PC$_{60}$BM.[27, 28]

The efficiency of free charge generation in organic solar cells is crucial for the overall power conversion efficiency of the solar cell device. The detailed mechanism, however, is still under debate and more complex than simple diffusion of charges from the interface to the bulk after charge transfer. Accordingly, several different pictures have been suggested to explain the astonishingly high efficiency of charge separation in organic bulk heterojunctions.

Very recently, Gélinas et al.[29] demonstrated long-range charge separation over a distance of 4 nm on a timescale as short as 40 fs. In fact, at this distance the mutual Coulomb attraction between electron and hole is significantly lowered and the remaining attraction may be overcome by additional driving forces such as energy differences between the disordered interface and more ordered bulk, energy level bending due to interfacial dipoles or other effects.[30] Gélinas et al. emphasized the importance of charge delocalization in fullerene clusters which facilitates ultrafast long-range charge separation.

The necessity of the concept of delocalization to ensure ultrafast charge separation is, however, debated and the ultrafast and very efficient charge separation may alternatively be explained by the high carrier mobility (1-10 cm²/Vs) observed directly after exciton dissociation. In fact, it was recently demonstrated by Kinetic Monte Carlo (KMC) simulations, that the high local charge carrier mobility typically determined on bulk heterojunctions by ultrafast time-resolved THz measurements[31] enables fast electron-hole pair separation over distances sufficiently large to overcome the Coulomb attraction.[22, 23, 32] For instance, Esenturk et al. determined a lower limit of the mobility for holes in P3HT of 1 cm^2/Vs.[33] Static disorder at the interface as well as entropy changes are also discussed as

additional driving forces aiding charge separation.[34, 35] The issue of the charge separation and recombination mechanism and its correlation with charge carrier mobility and disorder at the interface has recently been addressed for PCDTBT:PC$_{60}$BM by Howard *et al.*[36] without involving any coherent processes. The authors showed that charge separation is facilitated by an initially high, non-equilibrium mobility and relaxation within the density of states results in fast hopping of charges away from the interface.

A third concept used to explain the high efficiency of charge separation is the existence of an energy cascade between the pure and mixed phases in the BHJ morphology. It has been found that there is an energetic offset between the pure and mixed phases of polymer:fullerene BHJs due to both differences in molecular aggregation,[7, 21] and due to the presence of intermolecular interactions between the polymer and fullerene at the molecular interface.[20] These energetic offsets have been found to enhance charge separation efficiency both experimentally[21] and in Kinetic Monte Carlo simulations.[22, 23] The energetic offsets enhance charge separation efficiency by producing a driving force for charges to move from the mixed phase into the pure phase. Once charges encounter an energetic offset they are efficiently moved into the pure phase from the mixed phase and prevented from returning to the mixed phase, allowing them to be transported away from the polymer:fullerene interface and reducing their likelihood of recombination.

In summary, all concepts used to explain the high efficiency of charge separation observed in several polymer:fullerene blends have in common that an electron-hole separation of about 4-5 nm[22, 29] is required to overcome the Coulomb binding energy at room temperature. However, they differ in the exact nature of the process of charge separation, that is, whether delocalization across neighboring molecules is a necessary prerequisite for efficient charge separation, whether an initially high charge carrier mobility is sufficient to ensure efficient charge separation, or whether the presence of an energetic offset between the pure and mixed phases is required to ensure charge separation.

4. Conclusions

In the present work we show that solar cells prepared from pBTTT:PC$_{70}$BM at a donor-acceptor ratio of 1:1 exhibit mainly sub-ns geminate recombination after exciton dissociation. The free carrier generation yield is, however, significantly improved by changing the donor-acceptor ratio to 1:4 which introduces extended fullerene domains and thus percolation paths for the charge carriers. In fact, the efficiency of separation on the sub-nanosecond timescale is greatly enhanced by this morphological difference, indicating that extended fullerene domains are not only important as extraction pathways for free charge carrier, but also play a key role during the charge separation process. This finding is compatible with the aforementioned concepts, as the charge separation can be facilitated either by delocalization over fullerene aggregates or by a high initial charge carrier mobility plus an energy offset between mixed and pure phases. Hence, further experiments are necessary to address this issue and to obtain a conclusive picture of the underlying physics of charge separation in polymer:fullerene blends.

Supporting Information

Supporting Information is available from the Wiley Online Library or from the author.

Acknowledgements

[1]   Y. Liu, C.-C. Chen, Z. Hong, J. Gao, Y. Yang, H. Zhou, L. Dou, G. Li, *Sci. Rep.* **2013**, *3*, 3356.
[2]   M. A. Green, K. Emery, Y. Hishikawa, W. Warta, E. D. Dunlop, *Prog. Photovolt. Res. Appl.* **2014**, *22*, 1.
[3]   J.-L. Brédas, D. Beljonne, V. Coropceanu, J. Cornil, *Chem. Rev.* **2004**, *104*, 4971.
[4]   Y. Kim, S. Cook, S. M. Tuladhar, S. A. Choulis, J. Nelson, J. R. Durrant, D. D. C. Bradley, M. Giles, I. McCulloch, C.-S. Ha, M. Ree, *Nat. Mater.* **2006**, *5*, 197.
[5]   H. Mangold, A. A. Bakulin, I. A. Howard, C. Kastner, D. A. M. Egbe, H. Hoppe, F. Laquai, *Phys. Chem. Chem. Phys.* **2014**, *16*, 20329.
[6]   Y. Tamai, K. Tsuda, H. Ohkita, H. Benten, S. Ito, *Phys. Chem. Chem. Phys.* **2014**, *16*, 20338.
[7]   F. C. Jamieson, E. B. Domingo, T. McCarthy-Ward, M. Heeney, N. Stingelin, J. R. Durrant, *Chem. Sci.* **2012**, *3*, 485.
[8]   N. C. Miller, S. Sweetnam, E. T. Hoke, R. Gysel, C. E. Miller, J. A. Bartelt, X. Xie, M. F. Toney, M. D. McGehee, *Nano Lett.* **2012**, *12*, 1566.
[9]   C. Schwarz, H. Bässler, I. Bauer, J.-M. Koenen, E. Preis, U. Scherf, A. Köhler, *Adv. Mater.* **2012**, *24*, 922.
[10]   W. L. Rance, A. J. Ferguson, T. McCarthy-Ward, M. Heeney, D. S. Ginley, D. C. Olson, G. Rumbles, N. Kopidakis, *ACS Nano* **2011**, *5*, 5635.
[11]   D. M. Guldi, C. Luo, M. Prato, A. Troisi, F. Zerbetto, M. Scheloske, E. Dietel, W. Bauer, A. Hirsch, *J. Am. Chem. Soc.* **2001**, *123*, 9166.
[12]   E. H. A. Beckers, S. C. J. Meskers, A. P. H. J. Schenning, Z. Chen, F. Würthner, P. Marsal, D. Beljonne, J. Cornil, R. A. J. Janssen, *J. Am. Chem. Soc.* **2005**, *128*, 649.
[13]   J. A. Bartelt, Z. M. Beiley, E. T. Hoke, W. R. Mateker, J. D. Douglas, B. A. Collins, J. R. Tumbleston, K. R. Graham, A. Amassian, H. Ade, J. M. J. Fréchet, M. F. Toney, M. D. McGehee, *Adv. Energy Mater.* **2013**, *3*, 364.
[14]   K. Schmidt, C. J. Tassone, J. R. Niskala, A. T. Yiu, O. P. Lee, T. M. Weiss, C. Wang, J. M. J. Fréchet, P. M. Beaujuge, M. F. Toney, *Adv. Mater.* **2014**, *26*, 300.
[15]   B. A. Collins, Z. Li, J. R. Tumbleston, E. Gann, C. R. McNeill, H. Ade, *Adv. Energy Mater.* **2013**, *3*, 65.
[16]   M. Scarongella, A. A. Paraecattil, E. Buchaca-Domingo, J. D. Douglas, S. Beaupre, T. McCarthy-Ward, M. Heeney, J. E. Moser, M. Leclerc, J. M. J. Frechet, N. Stingelin, N. Banerji, *J. Mater. Chem. A* **2014**, *2*, 6218.
[17]   N. C. Cates, R. Gysel, Z. Beiley, C. E. Miller, M. F. Toney, M. Heeney, I. McCulloch, M. D. McGehee, *Nano Lett.* **2009**, *9*, 4153.
[18]   I.-W. Hwang, J. Young Kim, S. Cho, J. Yuen, N. Coates, K. Lee, M. Heeney, I. McCulloch, D. Moses, A. J. Heeger, *J. Phys. Chem. C* **2008**, *112*, 7853.

[19] A. Zusan, K. Vandewal, B. Allendorf, N. H. Hansen, J. Pflaum, A. Salleo, V. Dyakonov, C. Deibel, *Adv. Energy Mater.* **2014**, doi: 10.1002/aenm.201400922.

[20] S. Sweetnam, K. R. Graham, G. O. Ngongang Ndjawa, T. Heumüller, J. A. Bartelt, T. M. Burke, W. Li, W. You, A. Amassian, M. D. McGehee, *J. Am. Chem. Soc.* **2014**, *136*, 14078.

[21] S. Shoaee, S. Subramaniyan, H. Xin, C. Keiderling, P. S. Tuladhar, F. Jamieson, S. A. Jenekhe, J. R. Durrant, *Adv. Funct. Mater.* **2013**, *23*, 3286.

[22] T. M. Burke, M. D. McGehee, *Adv. Mater.* **2014**, *26*, 1923.

[23] C. Groves, *Energy Environ. Sci.* **2013**, *6*, 1546.

[24] F. Etzold, I. A. Howard, R. Mauer, M. Meister, T.-D. Kim, K.-S. Lee, N. S. Baek, F. Laquai, *J. Am. Chem. Soc.* **2011**, *133*, 9469.

[25] *See supplementary material at for details*.

[26] S. Gélinas, A. Rao, A. Kumar, S. L. Smith, A. W. Chin, J. Clark, T. S. van der Poll, G. C. Bazan, R. H. Friend, *Science* **2013**, 512.

[27] I. A. Howard, R. Mauer, M. Meister, F. Laquai, *J. Am. Chem. Soc.* **2010**, *132*, 14866.

[28] F. Etzold, I. A. Howard, N. Forler, D. M. Cho, M. Meister, H. Mangold, J. Shu, M. R. Hansen, K. Müllen, F. Laquai, *J. Am. Chem. Soc.* **2012**, *134*, 10569.

[29] S. Gélinas, A. Rao, A. Kumar, S. L. Smith, A. W. Chin, J. Clark, T. S. van der Poll, G. C. Bazan, R. H. Friend, *Science* **2014**, *343*, 512.

[30] M. Schrader, R. Fitzner, M. Hein, C. Elschner, B. Baumeier, K. Leo, M. Riede, P. Bäuerle, D. Andrienko, *J. Am. Chem. Soc.* **2012**, *134*, 6052.

[31] N. Vukmirović, C. S. Ponseca, H. Němec, A. Yartsev, V. Sundström, *J. Phys. Chem. C.* **2012**, *116*, 19665.

[32] M. L. Jones, R. Dyer, N. Clarke, C. Groves, *Phys. Chem. Chem. Phys.* **2014**, *16*, 20310.

[33] O. Esenturk, J. S. Melinger, E. J. Heilweil, *J. Appl. Phys.* **2008**, *103*.

[34] T. M. Clarke, J. R. Durrant, *Chem. Rev.* **2010**, *110*, 6736.

[35] B. A. Gregg, *J. Phys. Chem. Lett.* **2011**, *2*, 3013.

[36] I. A. Howard, F. Etzold, F. Laquai, M. Kemerink, *Adv. Energy Mater.* **2014**, *4*, doi: 10.1002/aenm.201301743.

Chart 1. Chemical structures of pBTTT-C14 and PC$_{70}$BM as well as a schematic representation of the film morphology for blends using a 1:1 and 1:4 donor:acceptor ratio.
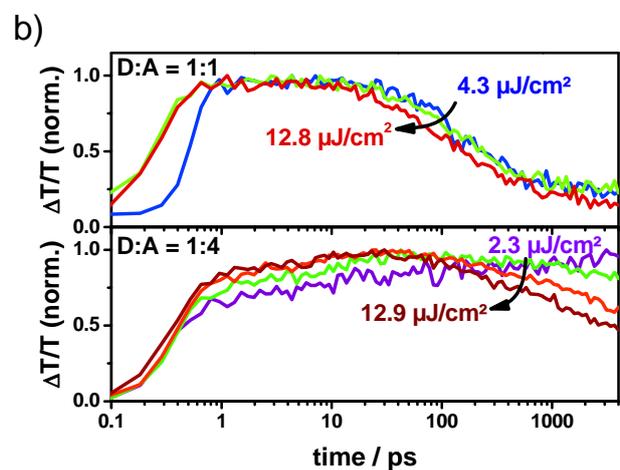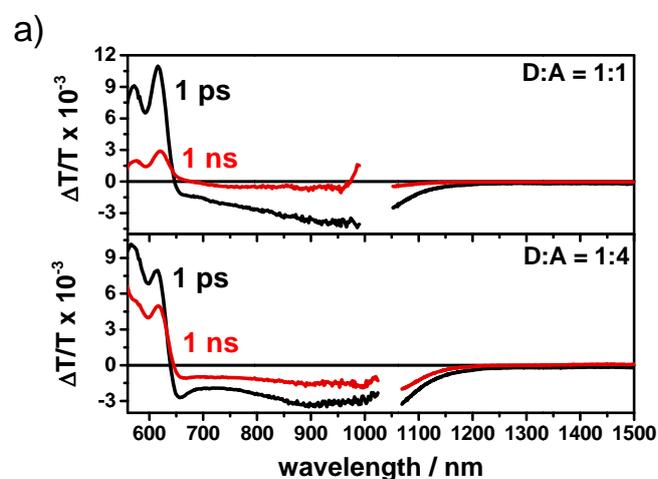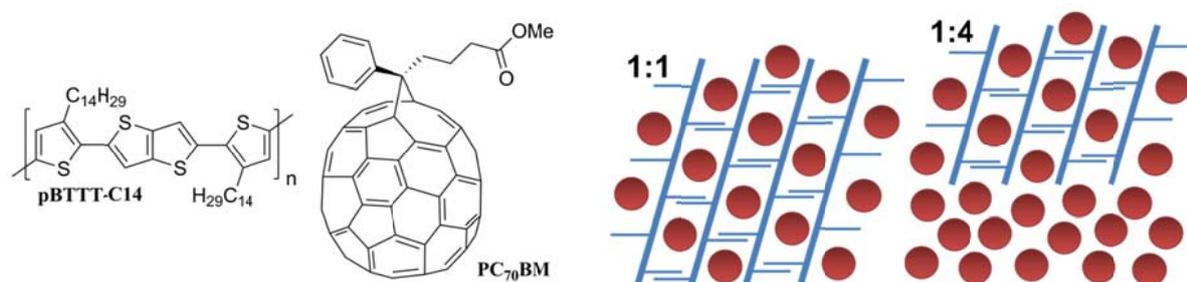

Figure 1. (a) ps-ns TA spectra of a pBTTT:PC$_{70}$BM thin film blend with a donor-acceptor ratio of 1:1 (upper panel, 11.2 µJ/cm²) and 1:4 (lower panel, 8.7 µJ/cm²). (b) ground-state bleaching kinetics of a pBTTT:PC$_{70}$BM 1:1 blend (upper panel, 610-635 nm) and a 1:4 blend (lower panel, 585-605 nm) at different excitation intensities.
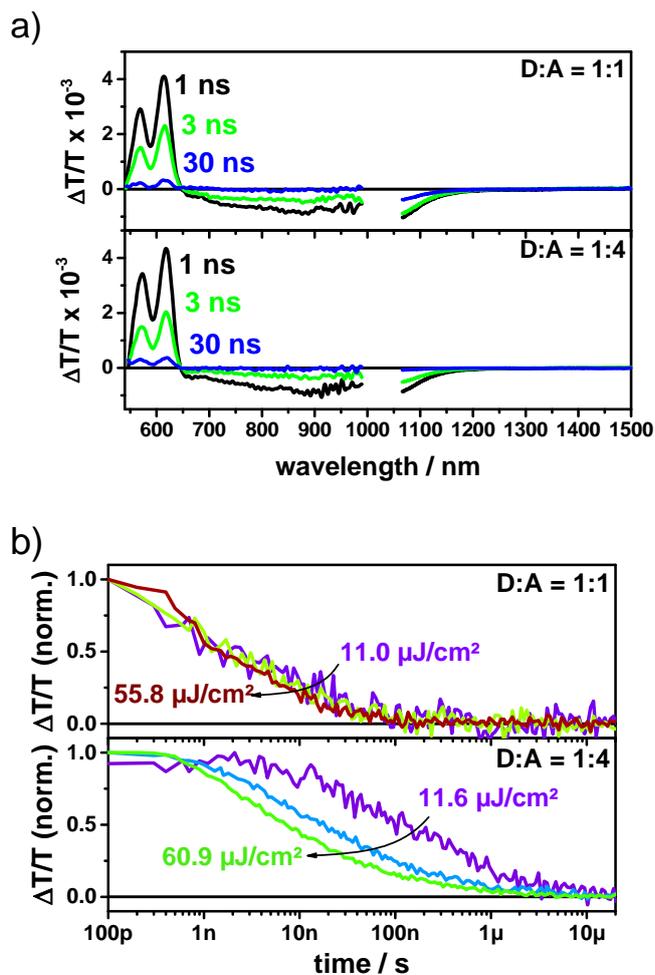
Figure 2. (a) ns-µs TA spectra of thin film blends of pBTTT:PC$_{70}$BM with a donor-acceptor ratio of 1:1 (upper panel, 28.3 µJ/cm²) and 1:4 (lower panel, 52.7 µJ/cm²). (b) ground-state bleaching kinetics of the same pBTTT:PC$_{70}$BM 1:1 (upper panel, 610-630 nm) and 1:4 blend (lower panel, 610-630 nm) at different excitation densities.
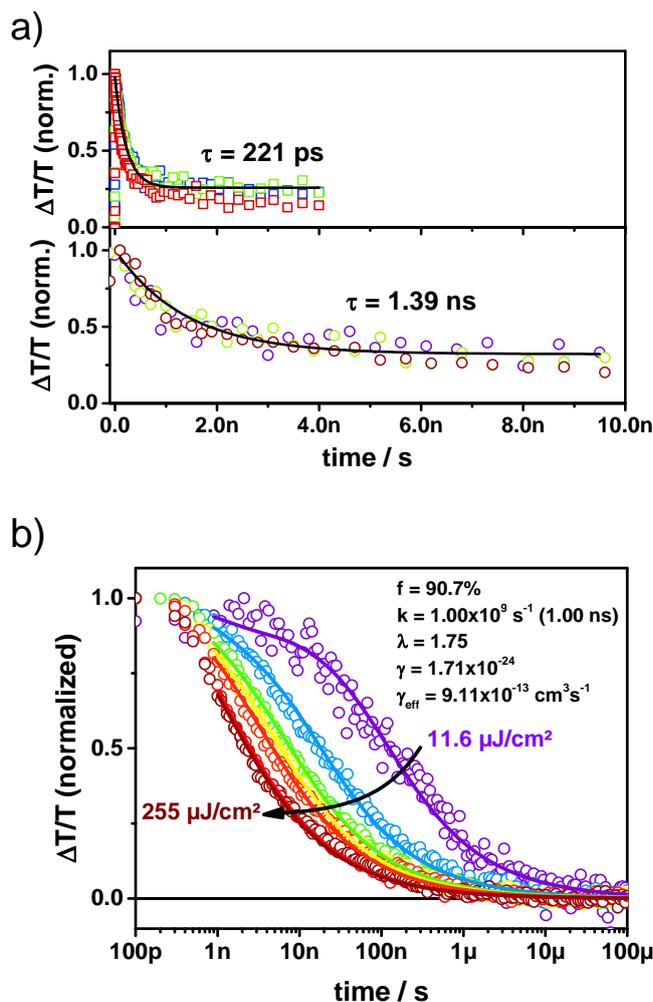
Figure 3. (a) Monoexponential fit (black solid line) to the ground-state bleaching dynamics (open symbols) of a pBTTT:$PC_{70}BM$ (1:1) thin film blend to the ps-ns dynamics (upper panel, 610-635 nm) and ns-μs dynamics (lower panel, 610-630 nm). (b) Intensity dependence of the ns-μs decay dynamics of the ground-state bleaching of a pBTTT:$PC_{70}BM$ (1:4) blend (open symbols, 610-630 nm) and fit to a two pool model (solid lines). The inset depicts the obtained fitting parameters describing the experimentally-measured decay dynamics.

Table 1. Photovoltaic parameters of pBTTT:$PC_{70}BM$ solar cells at donor-acceptor ratios of 1:1 and 1:4.

D:A ratio	V_{OC} [V]	I_{SC} [mA cm^{-2}]	FF	PCE [%]
1:1	0.5	2.6	0.43	0.55
1:4	0.5	8.3	0.50	2.4

The phase separation determines the carrier dynamics in pBTTT:PC$_{70}$BM photovoltaic blends as shown by pump-probe spectroscopy. The exclusive formation of cocrystals in 1:1 blends leads to sub-ns geminate recombination of CT states, while in 1:4 blends, in which extended fullerene domains exist in addition to the cocrystal phase, charge separation is facilitated and free carriers undergo non-geminate recombination.

Dominik W. Gehrig, Ian A. Howard, Sean Sweetnam, Tim M. Burke, Michael D. McGehee, Frédéric Laquai*

The Impact of Donor-Acceptor Phase Separation on the Charge Carrier Dynamics in pBTTT:PCBM Photovoltaic Blends